Hydrol. Earth Syst. Sci. Discuss., 7, 5467–5496, 2010
www.hydrol-earth-syst-sci-discuss.net/7/5467/2010/
doi:10.5194/hessd-7-5467-2010

Hydrology and Earth System Sciences Discussions

On the sampling distribution of the coefficient of L-variation for hydrological applications

A. Viglione

Institut für Wasserbau und Ingenieurhydrologie, Technische Universität Wien, Wien, Austria

Received: 27 July 2010 – Accepted: 3 August 2010 – Published: 10 August 2010

Correspondence to: A. Viglione (viglione@hydro.tuwien.ac.at)

Published by Copernicus Publications on behalf of the European Geosciences Union.

Abstract

The coefficient of L-variation (L-CV) is commonly used in statistical hydrology, in particular in regional frequency analysis, as a measure of steepness of the frequency curve. The aim of this work is to infer the full frequency distribution of the sample L-CV (and, consequently, its confidence intervals) for small samples and without making assumptions on the underlying parent distribution of the hydrological variable of interest. Several two-parameters candidate distributions are compared for a wide range of cases using Monte-Carlo simulations. A distribution-free method, recently proposed to estimate the variance structure of sample L-moments, is used to provide the parameters for the candidate distributions. It is shown that the log-Student t distribution approximates best, in most of the cases, the distribution of the sample L-CV and that a simple correction of the bias for the sample L-CV and its variance improves the fit. Also, the parametric method proposed here is demonstrated to perform better than the non-parametric bootstrap. An example of how this result could be used in hydrology is presented, namely in the comparison of methods for regional flood frequency analysis.

1 Introduction

It is well known that the sample coefficient of variation (CV), i.e., the ratio of standard deviation to the mean of a series of data, exhibits substantial bias and variance when samples are small or belong to highly skewed populations (Vogel and Fennessey, 1993). This is the problem that is normally encountered in hydrology when dealing with floods or extreme rainfall events. The coefficient of L-variation (L-CV) is another – more efficient in many cases – measure of data dispersion introduced by Hosking (1990). It has hence replaced the conventional CV in various applications of statistical hydrology. In particular, the use of the L-CV as a measure of steepness of the flood frequency curve has become a standard in regional flood frequency analysis (see e.g. Pearson, 1991; Hosking and Wallis, 1993; Stedinger and Lu, 1995; Fill and Stedinger, 1998;

HESSD

7, 5467–5496, 2010

Sampling distribution of the coefficient of L-variation

A. Viglione

Hosking and Wallis, 1997; Robson and Reed, 1999; Castellarin et al., 2001). Many statistical procedures of regionalization of floods are based on the hypothesis that the L-CV is informative enough to represent the differences among the flood frequency distributions at different sites. For example, the sample L-CV is used to designate "homogeneous regions", where it is assumed that the frequency distribution of flood peaks for different sites is the same, except for a site-specific scale factor (Dalrymple, 1960, Index-Flood method). Other studies state that the slope of the flood frequency curves (or, equivalently, their L-CV) should be taken as the statistical descriptor to be related to catchment attributes such as area or mean elevation (see e.g. Robinson and Sivapalan, 1997; Allamano et al., 2009).

In this work we are interested in the estimation of the sampling distribution of the L-CV, i.e., the probability distribution of the sample L-CV. The possibility to infer this distribution would allow one to know the range in which the L-CV of a sample is included at a given level of probability (i.e., the confidence interval) rather than to represent it by a single number. It would also provide a means to formulate homogeneity and goodness-of-fit test statistics for regional frequency analysis.

In the asymptotic distribution theory, approximate estimates of the sampling distribution of the L-CV are derived for relatively long samples and for particular underlying parent distributions (see e.g. Hosking, 1986, 1990). In the hydrological literature some attempts to extend the asymptotic results to shorter samples exist. For example, Chowdhury et al. (1991) assume that the sample L-CV is normally distributed and use a first-order estimate of its asymptotic variance corrected, for small samples, with coefficients obtained through a Monte-Carlo procedure. In their analysis a Generalized Extreme Value parent distribution is assumed. Sankarasubramanian and Srinivasan (1999) consider, in a similar work, the Generalized Normal, Log-Normal and Pearson type III distributions.

The objective of this work is to infer the sampling distribution of the L-CV for short samples and independently of the underlying parent distribution. We exploit the results of a distribution-free approach, recently proposed by the statistical community, to derive estimators for variances and covariances of sample L-moments (Elamir and Seheult, 2004). The estimators of the mean and variance of the sample L-CV are used to fit several two-parameters candidate distributions (Sect. 2). They are compared for a wide range of sample lengths and underlying parent distributions through goodness-of-fit techniques. We use a graphical goodness-of-fit method that is able to evidence the reasons for the lack of fit of the candidate distribution, in particular the effects of bias of estimation of mean and variance of the sample L-CV, and a standard goodness-of-fit measure, the Anderson-Darling test statistic (Sect. 3). The results are shown in Sect. 4 where, in addition: (i) a correction for the bias of estimation of mean and variance of the sample L-CV is proposed (Sect. 4.1); (ii) the method is compared to the non-parametric bootstrap, an appealing computer-based alternative method (Sect. 4.2); and (iii) the goodness of estimation of the 90% confidence intervals for the sample L-CV is checked.

The outcome of this study for hydrological applications is shown through an example (Sect. 5) in which different regionalization techniques (the index-flood technique with "fixed regions", the "region of influence" approach and a "region-free" simple regression method) are compared against a given data-set of flood peaks. Their performance is assessed by counting how often the L-CV confidence interval actually includes the regionally estimated L-CV.

2 Sampling distribution of the L-CV

L-moments were introduced by Hosking (1990) and are linear combinations of the Probability Weighted Moments defined by Greenwood et al. (1979) (see also Sillitto, 1969). Sample Probability Weighted Moments, computed from the order statistics $X_{1:n}, X_{2:n}, \ldots X_{n:n}$, are given by

$$b_k = n^{-1} \binom{n-1}{k}^{-1} \sum_{j=k+1}^{n} \binom{j-1}{k} X_{j:n} \ , \tag{1}$$

HESSD
7, 5467–5496, 2010

where n is the sample length and k is the order of the probability weighted moment. Sample L-moments are defined as

$$l_r = \sum_{k=0}^{r-1} p^*_{r-1,k} b_k \quad , \tag{2}$$

where the coefficients

$$p^*_{r,k} = (-1)^{r-k} \binom{r}{k} \binom{r+k}{k} \tag{3}$$

are those of the "shifted Legendre polynomials" (see Hosking and Wallis, 1997). Since L-moment estimators are linear functions of the sample values, they should be virtually unbiased and have relatively small sampling variance.

The asymptotic variances and covariances of the sample L-moments $l_1, l_2, \ldots, l_n$ were derived by Hosking (1990), who also demonstrated that their distribution is asymptotically normal. Elamir and Seheult (2004) derive the exact variance structure of sample L-moments in the non-asymptotic case without formulating assumptions on the underlying parent distributions. Observing that Eq. (2) can also be expressed as $\mathbf{l} = \mathbf{b}\mathbf{C}^T$, where $\mathbf{l} = (l_1, \ldots, l_n)$, $\mathbf{b} = (b_0, \ldots, b_{n-1})$ and $\mathbf{C}$ is the $n \times n$ lower triangular matrix with entries $p^*_{r-1,k}$ given in Eq. (3), the variance matrix of the L-moments is given by

$$\mathrm{var}(\mathbf{l}) = \mathbf{C}\boldsymbol{\Theta}\mathbf{C}^T \tag{4}$$

where $\boldsymbol{\Theta} = \mathrm{var}(\mathbf{b})$ is the variance matrix of the probability weighted moments with elements $\theta_{kk} = \mathrm{var}(b_k)$ and $\theta_{kl} = \mathrm{cov}(b_k, b_l)$. Elamir and Seheult (2004) demonstrate that a distribution-free unbiased estimator of θ_{kl} is

$$\hat{\theta}_{kl} = b_k b_l - \frac{1}{n^{(k+l+2)}} \sum_{1 \le i < j \le n} [(i-1)^{(k)}(j-k-2)^{(l)} + \\ +(i-1)^{(l)}(j-l-2)^{(k)}] X_{i:n} X_{j:n} \quad , \tag{5}$$

HESSD
7, 5467–5496, 2010

Sampling distribution of the coefficient of L-variation

A. Viglione

where $n^{(r)} = n(n-1)\ldots(n-r+1)$. The matrix $\hat{\mathbf{\Theta}}$, obtained with $\hat{\theta}_{kl}$ given in Eq. (5), is then an unbiased estimator of the variance matrix $\mathbf{\Theta}$. On these basis, it descends from Eq. (4) that an unbiased estimator of var(**l**) is simply:

$$\widehat{\mathrm{var}(\mathbf{l})} = \mathbf{C}\hat{\mathbf{\Theta}}\mathbf{C}^T \quad . \tag{6}$$

The sample L-CV, i.e., the coefficient of L-variation, is defined by the ratio of the first two sample L-moments,

$$t = l_2/l_1 \quad , \tag{7}$$

where l_1 is the sample mean and l_2 is a measure of the dispersion around the mean value. The variance of the L-moment ratio t can be related to the variance structure of sample L-moments given in Eq. (6) using a Taylor-series-based approximation to the variance of the ratio of two random variables (see e.g. Kendall and Stuart, 1961–1979):

$$\widehat{\mathrm{var}(t)} \cong \left[\frac{\widehat{\mathrm{var}(l_1)}}{l_1^2} + \frac{\widehat{\mathrm{var}(l_2)}}{l_2^2} - 2\frac{\widehat{\mathrm{cov}(l_1,l_2)}}{l_1 l_2}\right]\left[\frac{l_2}{l_1}\right]^2 \quad . \tag{8}$$

According to Hosking (1990), the L-moment ratio estimators are asymptotically normally distributed and have small bias and variance, specially if compared with the classical coefficients of variation, skewness and kurtosis (Hosking and Wallis, 1997). Keeping the hypothesis of normality, formulated in the asymptotic theory, the first candidate distribution for the sample L-CV considered here is

$$t + \sqrt{\widehat{\mathrm{var}(t)}} \cdot N(0,1) \quad , \tag{9}$$

where $N(0,1)$ is the standard normal distribution. Because for short samples the normal distribution could be too narrow, inspired by the definition of the distribution of the mean of a sample when its real variance is unknown (see e.g. Kottegoda and Rosso, 1997), we also consider

$$t + \sqrt{\widehat{\mathrm{var}(t)}} \cdot T_{n-1} \quad , \tag{10}$$

HESSD
7, 5467–5496, 2010

where T_{n-1} is a Student t distribution with $n-1$ degrees of freedom (being n the sample length).

Both the normal and the Student t distribution are symmetric. On the other hand, given that in hydrology random variables are typically non-negative (e.g. Koutsoyiannis, 2005) some sampling distributions should be asymmetric. Therefore, we consider here also

$$G\left(k=\frac{t^2}{\widehat{\mathrm{var}(t)}},\ \phi=\frac{\widehat{\mathrm{var}(t)}}{t}\right) \quad , \tag{11}$$

where G is a gamma distribution with shape parameter k and scale parameter ϕ, whose density function is

$$f_G(x;k,\phi)=\frac{1}{\phi^k\Gamma(k)}x^{k-1}e^{-(x/\phi)} \quad . \tag{12}$$

Among the asymmetric distributions, we also consider the log-normal and the log-Student t distributions, i.e., we check if the logarithm of the sample L-CV are approximately normally or Student t distributed. In the first case, the sampling distribution of the logarithm of the L-CV can be approximated by

$$\log(t)-\frac{1}{2}\log\left(1+\frac{\widehat{\mathrm{var}(t)}}{t^2}\right)+ \\ +\sqrt{\log\left(1+\frac{\widehat{\mathrm{var}(t)}}{t^2}\right)}\cdot N(0,1) \quad , \tag{13}$$

which follows from the definition of mean and variance of a log-normally distributed random variable. Analogously, assuming that the same relationships hold for the log-Student t distribution, which is a reasonable approximation,

$$\log(t)-\frac{1}{2}\log\left(1+\frac{\widehat{\mathrm{var}(t)}}{t^2}\right)+$$

HESSD
7, 5467–5496, 2010

$$+\sqrt{\log\left(1+\frac{\widehat{\mathrm{var}(t)}}{t^2}\right)}\cdot T_{n-1} \quad . \tag{14}$$

The log-Student's t distribution is a generalization of the log-normal distribution that has heavier tails but approaches log-normality as the sample length n increases.

In the following we present the method used to verify how these approximations fit for samples of length n and several underlying parent distributions.

3 Goodness-of-fit method

The goodness of estimation of the distribution of sample L-CV can be tested through Monte-Carlo simulations. Given a parent distribution whose characteristics (and real L-CV τ) are known, $N = 10000$ samples are randomly extracted from it. For each of them, the estimates of the sample L-CV t and its variance $\widehat{\mathrm{var}(t)}$ are calculated as shown in Sect. 2. If the approximations of Eqs. (9–14) are reasonable, the probability of non-exceedance of τ should be uniformly distributed between 0 and 1. Therefore we test the uniformity of this probability, hereafter indicated as $P(\tau)$.

Many goodness-of-fit tests for the uniform distribution exist (e.g. D'Agostino and Stephens, 1986). As in Laio and Tamea (2007) we adopt here a less formal but more revealing graphical method, based on a probability plot representation. Given, for one candidate distribution, the sample $P_1(\tau), P_2(\tau), P_3(\tau), \ldots, P_N(\tau)$ resulting from the N Monte-Carlo simulations, the probability plot represents the $P_i(\tau)$ values versus their empirical cumulative distribution function, R_i/N. The shape of the resulting curve reveals if the sample of probabilities is approximately uniform, in which case the ($P_i(\tau)$, R_i/N) points are close to the bisector of the diagram. The graphical method allows to investigate which are the reasons for a lack of fit of a candidate distribution, in particular evidencing the effects of biases of estimation for t and $\widehat{\mathrm{var}(t)}$. In fact, the shape of the curves in the probability plot is suggestive of the encountered problem, since the steepness of the curves is larger where more $P_i(\tau)$ points concentrate (see Fig. 2 in Laio and Tamea, 2007). If the curve is over the bisector in the left part of the graph and under it in the right part, the $P_i(\tau)$ points are concentrated in the vicinity of the end points 0 and 1, which corresponds to have the τ value that falls, more frequently than expected, on the tails of the distributions. The chosen variances of the distributions are then too small. In the opposite case, when the curve has an S shape and crosses the bisector in the middle of the graph, the chosen variances are too high because the $P_i(\tau)$ points are concentrated in the vicinity of the middle value 0.5. When the curves are always over or under the bisector, then the scale parameters of the distribution (in this case t) have been overestimated or underestimated, respectively. In the first case the real τ value falls, more frequently than expected, on the low tail of the distributions, then the estimated t are too high, and viceversa.

In addition to the graphical method, we use the Anderson-Darling statistic in order to synthetically quantify the discrepancy between the cumulative distribution function (CDF) of $P_1(\tau), P_2(\tau), P_3(\tau), \ldots, P_N(\tau)$ and the uniform distribution U between 0 and 1. The Anderson-Darling statistic is a measure of the mean squared difference between the empirical and hypothetical CDF, in practice estimated as (e.g. D'Agostino and Stephens, 1986; Laio, 2004):

$$A^2 = -N - \frac{1}{N}\sum_{i=1}^{N}[(2i-1)\ln(U[P_i(\tau)]) + \\ +(2N+1-2i)\ln(1-U[P_i(\tau)])] \quad . \tag{15}$$

The best fit corresponds to the minimum value of A^2.

4 Results

To check the robustness of our approximations, many different situations are considered: we vary the length n of the samples, the underlying parent distribution and

HESSD
7, 5467–5496, 2010

Sampling distribution of the coefficient of L-variation

A. Viglione

its parameters. The considered parent distributions are: GEV (Generalized Extreme Value), P3 (Pearson type III), LN (Log-Normal with 3 parameters), GP (Generalized Pareto) and GL (Generalized Logistic). As in Viglione et al. (2007) we choose the parameters of these distributions by reference to the L-CV - L-CA (coefficient of L-skewness) space represented in Fig. 1 (the mean is taken equal to 1 without loss of generality) that is a reasonable space where the majority of hydrological (extreme value) samples falls (Vogel and Wilson, 1996; Viglione et al., 2007).

Some of the uniform probability plots of $P(\tau)$ are shown in Fig. 2, where the log-Student t distribution of Eq. (14) is the candidate distribution for t. In panel (a) samples are extracted from a GEV distribution with increasing asymmetry (from point A to point D of Fig. 1). It is evident that the log-Student t approximation works better for moderate asymmetry of the parent distribution than in the highly asymmetric cases. The approximation is good when the parent distribution is quasi-symmetric (point A) but not for very asymmetrical parent distributions (point C and D). In all cases the curve lie below the bisector, meaning that the estimate t is too low, specially in the right part of the graph, meaning that the upper tail of the distribution is too narrow. In panel (b) the parent distribution is Pearson Type III (P3). The goodness of the log-Student t approximation for the distribution of the L-CV is much less affected by the shape of the parent distribution when this is a P3. In this case, the approximation fits much better than in panel (a).

Similar conclusions can be derived from panels (c) and (d), that present the sensitivity of the log-Student t approximation to the length n of the samples (the parent distributions have, in this case, the same asymmetry, correspondent to point C of Fig. 1). As expected, for high n the goodness-of-fit of the candidate distribution increases. For very short samples ($n = 10$), in some few cases, the estimate $\widehat{\mathrm{var}(t)}$ of Elamir and Seheult (2004) is negative. In those cases, the Monte-Carlo simulations have been discarded when producing the curves in Fig. 2c and d. Therefore, the result for very short samples can be even worse than what shown in the figure.

HESSD

7, 5467–5496, 2010

Panels (e) and (f) show the uniform probability plots for different parent distributions in points A (low asymmetry) and D (high asymmetry). The behavior of the curves, specially in D, strongly depends on the underlying parent distribution. Considering high asymmetries (point D), the approximation of the sample L-CV distribution with moments t and $\widehat{\mathrm{var}(t)}$ is particularly bad for the GEV and GL distributions.

Similar plots (not shown here) have been produced for the other candidate distributions. The Normal and Student t distributions perform slightly better in the central part of the graph for small asymmetry (point A) and for the P3 parent distribution. Anyway the underestimation of the width of the upper tail is more marked than in the case of the asymmetric candidate distributions (gamma, log-Normal and log-Student). For all candidate distributions the shape of the curves are similar (below the bisector, specially for the upper right corner of the uniformity plots), meaning that, particularly for the GEV and GL parent distributions and for large asymmetries (point D), the estimators t and $\widehat{\mathrm{var}(t)}$ underestimate the true values. We consider this problem in the following subsection, where a distribution-free correction of these biases is proposed.

4.1 Bias correction

A simple bias correction for t and $s_t = \sqrt{\widehat{\mathrm{var}(t)}}$ can be obtained from Monte-Carlo simulations. Samples are generated for each combination of τ and τ_3 (gray points in Fig. 1), for each parent distribution (GEV, P3, LN, GP and GL) and for different sample lengths ($n = 10, 15, 20, 25, 30, 40, 50, 70, 100$). Given one simulation ($N = 1000$ samples), the bias of t is estimated as $\bar{t} - \tau$, where $\bar{t}$ is the arithmetic mean over N values of t and τ is the known L-CV of the parent distribution. In panel (a) of Fig. 3, we show how the bias of t, opportunely scaled with n (see e.g. Kendall and Stuart, 1961–1979, Sect. 17.10), increases for increasing asymmetry of the samples ($\bar{t}_3$ is the mean of the N sample L-skewness). Analogous results are obtained for the standard deviation of the sample L-CV (panel (b) of Fig. 3). The bias of s_t is evaluated as $(\bar{s}_t - \sigma_t)/\bar{s}_t$, where we assume $\sigma_t = \sqrt{(\sum_{i=1}^{N}(t_i - \bar{t})^2)/N}$ as the true standard deviations of the sample L-CV. In

HESSD
7, 5467–5496, 2010

both cases, the bias depends on the type of distribution: the P3 distribution shows the lowest bias and the GL distribution the largest, confirming the behavior in Fig. 2. Given one distribution, the scatter of the estimated biases for a fixed t_3 is mostly determined by the variability of the considered L-CV (grey points on vertical lines in Fig. 1) while the influence of the variability of sample lengths is highly reduced by the aforementioned scaling with n. Despite this effect of the variance of the parent distribution, we deem that the biases of t and s_t are substantially functions of n and t_3, along with the distribution type.

Using these Monte Carlo results in a pragmatic way, we propose the following simple corrections for the sample L-CV and its standard deviation:

$$t^{(c)} = \begin{cases} t + 3 \cdot t_3^{2.5}/n \text{ , if } t_3 > 0 \\ t \text{ , if } t_3 \leq 0 \end{cases} , \tag{16}$$

and

$$s_t^{(c)} = s_t \cdot (1 + 35 \cdot t_3^2/n) , \tag{17}$$

that are obtained with a non-linear regression approach (non linear least-squares). The curves corresponding to these corrections are represented in Fig. 3 as solid black lines. These corrections intentionally do not take into account the type of distribution because it is unknown in operational applications. It is important to stress again that the objective of this study is to approximate the sample distribution of the L-CV independently of the underlying (and unknown) parent distribution of the original variable, so to provide an operational tool.

As can be seen in Fig. 4, that is analogous to Fig. 2 but considers the adjustments of Eqs. (16) and (17), the corrections generally improve the results of the uniformity tests for highly asymmetric distributions. Some problems remain for very short samples ($n = 10$) and some parent distributions, but they are generally reduced. Similar results are obtained for the other candidate distributions. A synthetic comparison of these results is shown in Table 1, where the values of the Anderson-Darling statistic is shown

HESSD
7, 5467–5496, 2010

for the cases of Fig. 4. In most of the cases, the A^2 statistic is lower when the log-Student t distribution is assumed. Therefore, among the considered candidates, we select the log-Student t as the best approximation of the distribution of the sample L-CV.

4.2 The bootstrap approach

The parametric strategy is not the only possibility. As an alternative, the non-parametric bootstrap procedure can be used to make inference on t (estimating for example its confidence intervals) without making assumption on its distribution.

The bootstrap is a computer-based method for assigning measures of accuracy to statistical estimates. It was first introduced in the context of non parametric analysis of independent and identically distributed samples (Efron, 1979), but much research into its use in more complicated settings followed (see e.g. Davison and Hinkley, 1997, as a reference). The basic idea behind the non-parametric bootstrap is very simple. Given a sample and a statistic estimated on it (for example t), a bootstrap sample of the same size is drawn "with replacement" from the original one. Corresponding to a bootstrap sample is a bootstrap replication t^* of the statistic t. The bootstrap algorithm works by drawing many independent bootstrap samples (say $R = 2000$), evaluating the corresponding bootstrap replications, and estimating the standard error of t by the empirical standard deviation of the replications.

Many aspects of the behavior of the selected statistic can be measured with bootstrap, for example its confidence intervals. The standard method consists in using the standard normal confidence intervals, or the Student t confidence intervals, with the standard deviation obtained with the bootstrap. This method rely on the hypotheses that the distribution of the bootstrap replications (i.e., t^*) is unbiased and nearly normal. These hypotheses can be relaxed using the percentile method: obtaining the confidence intervals of t from the empirical percentiles of the sample of bootstrap replications t^*. This method can be improved further with the *bias-corrected and accel-*

HESSD
7, 5467–5496, 2010

erated (BC_a) bootstrap method. The BC_a intervals are more complicated to define than the percentile intervals (see e.g. Efron and Tibshirani, 1993, for a formal definition), but almost as easy to use.

Naturally, if one can obtain the confidence intervals of the estimate t for every level of probability, its sampling distribution is automatically defined. Given the definition of BC_a intervals in Efron and Tibshirani (1993, pages 184-188), the derivation of a non-parametric distribution of t can be performed quite easily. If $P^*(\tau)$ is the probability of non exceedance of τ on the bootstrap distribution of t, according to the BC_a method the corrected probability is

$$P(\tau) = \Phi\left[-\frac{\hat{a}\cdot\hat{z}_0^2 + (-\hat{a}\cdot\Phi^{-1}[P^*(\tau)] - 2)\cdot\hat{z}_0 + \Phi^{-1}[P^*(\tau)]}{\hat{a}\cdot\hat{z}_0 - \hat{a}\cdot\Phi^{-1}[P^*(\tau)] - 1}\right], \tag{18}$$

where $\Phi[.]$ is the standard normal cumulative distribution function, $\Phi^{-1}[.]$ is the percentile point on a standard normal distribution and the values of the bias correction $\hat{z}_0$ and the acceleration $\hat{a}$ can be computed as indicated in Efron and Tibshirani (1993, page 186).

The uniformity plot introduced in Sect. 3 has been applied to check if t approximately follows the calculated BC_a distribution of Eq. (18). As shown in Fig. 5, the bias of the central part of the curves indicates a significant overestimation of the mean value of the distribution of the sample L-CV. Moreover some of the curves, specially those correspondent to high asymmetry and small sample length, are "reverse S" shaped, meaning that the variance of the distribution is underestimated. The comparison between Figs. 5 and 4 confirms the better performance of our parametric method.

4.3 Confidence intervals

As was shown in Table 1, in most of the cases the log-Student t distribution gives the best approximation of the distribution of the sample L-CV. Since the Anderson-Darling statistic gives more weight to the tails of the distribution than to the central part of it, the log-Student t distribution is expected to be the best choice when calculating the confidence intervals for the sample L-CV. Here we check the goodness of the 90% confidence intervals of t using different candidate distributions in the corrected case, where the corrections of Eqs. (16) and (17) are applied to t and s_t, and using the BC_a non-parametric bootstrap. Table 2 shows the percentage of trials (which are 10000) in which the true value τ was not comprised into the confidence interval of t on the left or right side. The target miscoverage is 5% on each side: P_{05} and P_{95} are the probabilities that τ is lower than the 0.05 or greater than the 0.95 quantiles of the distribution of t (we expect that both P_{05} and P_{95} equal 5%). Among all the considered situations, Table 2 shows the cases considered already in Table 1 and Figs. 2, 4 and 5.

When using the parametric method, P_{05} is often slightly lower than 5% and P_{95} is almost often slightly higher than 5%, which means that the confidence intervals estimated in this way are a little too large for the left tail and too narrow for the right tail of the distribution of t. This problem is particularly evident for large asymmetries of the parent distribution and for small sample sizes, as was already evident in Fig. 4. The log-Student t approximation generally outperforms the others, i.e., the confidence intervals are better centered (both P_{05} and P_{95} are close to the ideal value 5%). The BC_a intervals for t ($R = 2000$ has been used) have a different behavior: P_{05} is always higher than 5% and in many cases higher than P_{95}, which is a consequence of the overestimation of the mean value of the distribution of the sample L-CV shown in Fig. 5. Despite its great time demand, the bootstrap performs in most of the cases worse than the corrected parametric method.

5 An application

The possibility to provide information on the distribution of the sample L-CV is relevant for hydrological applications. Here we show, in a simplified way, how confidence intervals for the sample L-CV could be used to analyse and compare the outcome of different regionalization methods. Following Hosking and Wallis (1997) cluster analysis can be used to define homogeneous disjoint regions whose samples should have the same L-CV. On the other hand one can use the region of influence (ROI) approach (Burn, 1990), or allow the continuous variability of L-CV (Robinson and Sivapalan, 1997), by estimating it with linear or non-linear regressions. All these different approaches can be compared using confidence intervals in an intuitive way.

Here we use the UK data available with the Flood Estimation Handbook (Robson and Reed, 1999). For every regionalization technique, morphoclimatic variables should be used to pool the sites. For simplicity, we suppose that the mean annual rainfall alone (indicated as SAAR) may explain the difference of the at-site flood frequency distributions, and that this difference is completely reflected in the coefficient of L-variation. Fig. 6 shows in a simple way how four methods of estimation of the regional L-CV can be compared. Mean annual precipitation is plotted against the bias-corrected L-CV. Gray circles have confidence intervals that contain the modeled regional L-CV while black crosses do not (the significance level is $\alpha = 0.10$; the assumed distribution for the sample L-CV is log-Student t with moments corrected using Eqs. (16) and (17). In panel (a) only one region is considered with a unique regional L-CV, here called t^R, given by the sample mean of all the sample-corrected $t^{(c)}$. If the confidence intervals are correctly estimated, the percentage P_{05} of sites for which the modeled t^R is below the confidence intervals of t should be equal to 5%, as well as P_{95}, i.e., the percentage of sites for which the modeled t^R is above the confidence intervals of t. In panel (a) $P_{05} = 15\%$ and $P_{95} = 27\%$, i.e., $P_{05} + P_{95} = 42\% \gg \alpha$, which means that the model is inappropriate and/or the chosen parameter (SAAR) does not explain completely the variability of the L-CV.

If one subdivides the sites in 3 regions using a clustering method, as in panel (b), the values of P_{05} and P_{95} decrease ($P_{05} = 12\%$ and $P_{95} = 25\%$). This means that the model is more appropriate than the previous one. With a region of influence approach (panel c), one obtains $P_{05} = 12\%$ and $P_{95} = 23\%$. In this case, for simplicity, a simplified ROI approach has been used, that assigns to each site the average of the L-CV of the most similar 20 sites in terms of SAAR. Finally, in panel (d) a linear regression between $t^{(c)}$ and SAAR is shown. The result ($P_{05} = 12\%$ and $P_{95} = 24\%$) is very similar to the three regions and ROI clustering methods. It is important to note that the high discordance between P_{05} and P_{95} and the theoretical value of 5% is not due to the approximation of the confidence intervals, for which we would expect uncertainties of the order of those in Table 2. This discordance is due to the fact that the data are not uniform, that SAAR is not sufficient to explain the regional variability of L-CV, that the regional methods are approximate, etc. Lower values of P_{05} and P_{95} would be obtained by using more catchment descriptors (not only SAAR) and more sophisticated techniques. The simple examples provided here intend to illustrate the method. They show that L-CV confidence intervals allow to analyse in a consistent way very different approaches as those based on site grouping and those that allow continuous variability of L-CV, for which standard techniques as homogeneity tests would be meaningless. Also, they provide a way to identify those sites that are "problematic" for the validity of the assumptions made (in the examples looking at the position of crosses and circles) and that should be further checked.

6 Conclusions

One of the most important concerns of Flood Frequency Analysis is the underlying distribution (or the lack of knowledge on its form, to be more precise) and the desire to lose the "distribution fetters" among hydrologists is really strong. Anyway the distribution-dependent methodologies dominate in practical hydrology, where distribution-free methods are seldom used. Recently Elamir and Seheult (2004) have provided a method to estimate the variance of sample L-moments and L-moment ratios without formulating assumptions on their parent distributions. This result is important and can prove to be very helpful in statistical hydrology, as the L-moments are extensively used. We use the estimators of Elamir and Seheult (2004) in this study. The focus is addressed to the coefficient of L-variation, which gives a measure of the dispersion of samples, and to its sampling distribution. We show that the log-Student t distribution is a valid candidate to represent the sampling distribution of the L-CV and, therefore, to derive its confidence intervals. A bias correction of the mean and variance of the sample L-CV substantially improves the fit of the log-Student t distribution to the simulated empirical distributions, particularly when the parent distribution of the samples is highly skewed. Even if the goodness-of-fit of this approximation still somewhat depends on the underlying parent distribution type (along with its asymmetry and the sample size), we deem that the good results shown in this paper demonstrate that the method can be very useful in practice, in particular for hydrological applications.

Acknowledgements. Financial support for the project "Mountain floods – regional joint probability estimation of extreme events" from the Austrian Academy of Sciences is acknowledged.

References

Allamano, P., Claps, P., and Laio, F.: An analytical model of the effects of catchment elevation on the flood frequency distribution, Water Resour. Res., 45(1), W01402, doi: 10.1029/2007WR006658, 2009. 5469

Burn, D. H.: Evaluation of regional flood frequency analysis with a region of influence approach, Water Resour. Res., 26(10), 2257–2265, 1990. 5482

Castellarin, A., Burn, D. H., and Brath, A.: Assessing the effectiveness of hydrological similarity measures for flood frequency analysis, J. Hydrol., 241, 270–285, 2001. 5469

Chowdhury, J. U., Stedinger, J. R., and Lu, L.: Goodness-of-fit tests for regional generalized extreme value flood distributions, Water Resour. Res., 27(7), 1765–1776, 1991. 5469

D'Agostino, R. and Stephens, M.: Goodness-of-fit techniques, Statistics: textBooks and monographs, 68, Department of Statistics, Southern Methodist University, Dallas, Texas, 1986. 5474, 5475

Dalrymple, T.: Flood frequency analyses, Water Supply Paper, 1543-A, US Geological Survey, Reston, Va., 1960. 5469

Davison, A. C. and Hinkley, D. V.: Bootstrap methods and their application, Cambridge University Press, Cambridge, 1997. 5479

Efron, B.: Bootstrap methods: another look at the jackknife, Ann. Stat., 7, 1–26, 1979. 5479

HESSD

7, 5467–5496, 2010

Sampling distribution of the coefficient of L-variation

A. Viglione

Efron, B. and Tibshirani, R.: An Introduction to the Bootstrap, Chapman & Hall, New York, 1993. 5480
Elamir, E. A. H. and Seheult, A. H.: Exact variance structure of sample l-moments, J. Stat. Plan. Inf., 124, 337–359, 2004. 5470, 5471, 5476, 5483
Fill, H. and Stedinger, J. R.: Using regional regression within index flood procedures and an empirical bayesian estimator, J. Hydrol., 210(1–4), 128–145, 1998. 5468
Greenwood, J., Landwehr, J., Matalas, N., and Wallis, J.: Probability weighted moments: Definition and relation to parameters of several distributions expressible in inverse form, Water Resour. Res., 15, 1049–1054, 1979. 5470
Hosking, J.: The theory of probability weighted moments, Tech. Rep. RC12210, IBM Research, Yorktown Heights, NY, 1986. 5469
Hosking, J.: L-moments: analysis and estimation of distributions using linear combinations of order statistics, J. Royal Statistical Soc., 52, 105–124, 1990. 5468, 5469, 5470, 5471, 5472
Hosking, J. and Wallis, J.: Some statistics useful in regional frequency analysis, Water Resour. Res., 29(2), 271–281, 1993. 5468
Hosking, J. and Wallis, J.: Regional Frequency Analysis: An Approach Based on L-Moments, Cambridge University Press, 1997. 5469, 5471, 5472, 5481, 5491
Kendall, M. and Stuart, A.: The Advanced Theory of Statistics, Charles Griffin & Company Limited, London, 1961–1979. 5472, 5477
Kottegoda, N. T. and Rosso, R.: Statistics, Probability, and Reliability for Civil and Environmental Engineers, international ed., 735 pp., McGraw-Hill Companies, 1997. 5472
Koutsoyiannis, D.: Uncertainty, entropy, scaling and hydrological stochastics. 1. marginal distributional properties of hydrological processes and state scaling, Hydrolog. Sci. J., 50(3), 381–404, 2005. 5473
Laio, F.: Cramer-von Mises and Anderson-Darling goodness of fit tests for extreme value distributions with unknown parameters, Water Resour. Res., 40, W09308, doi:10.1029/2004WR003204, 2004. 5475
Laio, F. and Tamea, S.: Verification tools for probabilistic forecasts of continuous hydrological variables, Hydrol. Earth Syst. Sci., 11, 1267–1277, doi:10.5194/hess-11-1267-2007, 2007. 5474, 5475
Pearson, C.: New zealand regional flood frequency analysis using l moments, J. Hydrol. (NZ), 30, 53–64, 1991. 5468
Robinson, J. and Sivapalan, M.: An investigation into the physical causes of scaling and het-

HESSD
7, 5467–5496, 2010

erogeneity of regional flood frequency, Water Resour. Res., 33(5), 1045–1059, 1997. 5469, 5482

Robson, A. J. and Reed, D. W.: Statistical procedures for flood frequency estimation, in Flood Estimation HandBook, vol. 3, p. 338, Institute of Hydrology Crowmarsh Gifford, Wallingford, Oxfordshire, 1999. 5469, 5482, 5496

Sankarasubramanian, A. and Srinivasan, K.: Investigation and comparison of sampling properties of l-moments and conventional moments, J. Hydrol., 218, 13–34, 1999. 5469

Sillitto, G.: Derivation of approximants to the inverse distribution function of a continuous univariate population from the order statistics of a sample, Biometrika, 56(3), 641–650, doi: 10.1093/biomet/56.3.641, 1969.) 5470

Stedinger, J. R. and Lu, L.: Appraisal of regional and index flood quantile estimators, Stoch. Hydrol. Hydraul., 9(1), 49–75, 1995. 5468

Viglione, A., Laio, F., and Claps, P.: A comparison of homogeneity tests for regional frequency analysis, Water Resour. Res., 43(3), W03428, doi:10.1029/2006WR005095, 2007. 5476, 5491

Vogel, R. M. and Fennessey, N.: L moment diagrams should replace product moment diagrams, Water Resour. Res., 29(6), 1745–1752, 1993. 5468

Vogel, R. M. and Wilson, I.: Probability distribution of annual maximum, mean, and minimum streamflows in the united states, J. Hydrol. Eng., 1(2), 69–76, 1996. 5476, 5491

Table 1. Anderson-Darling statistic of discrepancy between the CDF of 10 000 values of $P(\tau)$ from a Monte-Carlo experiment for five candidate distributions and the uniform distribution U. The corrections of Eqs. (16) and (17) are applied. The best fit is indicated by the bold font. Different situations are considered: **(a)** GEV parent distributions with different asymmetry (point A, B, C, D of Fig. 1); **(b)** P3 parent distributions with different asymmetry; **(c)** GEV parent distributions and samples of different length n; **(d)** P3 parent distributions and samples of different length n; **(e)** different parent distributions with low asymmetry (point A); **(f)** different parent distributions with high asymmetry (point D).

(a) GEV, $n = 30$

	normal	Student t	gamma	log-normal	log-Student t
A	33.2	23.6	21.9	23.2	**16.6**
B	53.8	42.3	43.7	46.6	**39.6**
C	91.6	75.4	79.0	83.1	**73.4**
D	226.2	191.4	209.2	212.9	**189.8**

(b) P3, $n = 30$

	normal	Student t	gamma	log-normal	log-Student t
A	21.3	16.0	14.0	16.7	**13.3**
B	31.1	22.0	15.9	14.0	**7.9**
C	27.9	21.4	10.6	5.9	**2.5**
D	50.6	41.2	29.3	16.3	**10.4**

(c) GEV, C

	normal	Student t	gamma	log-normal	log-Student t
$n = 100$	66.5	62.1	60.9	60.3	**56.7**
$n = 50$	95.1	84.0	85.4	85.5	**77.5**
$n = 30$	91.6	75.4	79.0	83.1	**73.4**
$n = 10$	296.8	**154.7**	226.5	243.5	171.1

HESSD

7, 5467–5496, 2010

Table 1. Continued

(d) P3, C					
	normal	Student t	gamma	log-normal	log-Student t
$n = 100$	7.3	6.5	3.2	2.3	**1.7**
$n = 50$	19.5	16.1	8.3	4.5	**2.2**
$n = 30$	27.9	21.4	10.6	5.9	**2.5**
$n = 10$	134.9	52.0	95.2	98.3	**47.9**
(e) $n = 30$, A					
	normal	Student t	gamma	log-normal	log-Student t
GEV	33.2	23.6	21.9	23.2	**16.6**
P3	21.3	16.0	14.0	16.7	**13.3**
LN	34.0	26.4	26.9	30.2	**25.2**
GP	45.5	39.2	40.2	39.2	**31.4**
GL	140.4	115.4	122.2	124.2	**107.8**
(f) $n = 30$, D					
	normal	Student t	gamma	log-normal	log-Student t
GEV	226.2	191.4	209.2	212.9	**189.8**
P3	50.6	41.2	29.3	16.3	**10.4**
LN	85.5	67.4	70.4	70.4	**59.4**
GP	46.3	33.4	28.6	23.3	**15.7**
GL	328.2	**283.9**	309.9	315.9	286.0

HESSD
7, 5467–5496, 2010

Table 2. Goodness of confidence intervals of t for the following candidate distributions: corrected parametric model with normal, Student t, gamma, log-normal and log-Student t distribution, bootstrap BC_a model with $R = 2000$. P_{05} and P_{95} are the percentage of trials (that are 10000) that the indicated interval missed the true value τ on the left or right side of the confidence interval. Different situations are considered: **(a)** GEV parent distributions with different asymmetry (point A, B, C, D of Fig. 1); **(b)** P3 parent distributions with different asymmetry; **(c)** GEV parent distributions and samples of different length n; **(d)** P3 parent distributions and samples of different length n; **(e)** different parent distributions with low asymmetry (point A); **(f)** different parent distributions with high asymmetry (point D).

(a) GEV, $n = 30$

	normal		Student t		gamma		log-normal		log-Student t		bootstrap BC_a	
	P_{05}	P_{95}	P_{05}	P_{95}	P_{05}	P_{95}	P_{05}	P_{95}	P_{05}	P_{95}	P_{05}	P_{95}
A	4.2	8.0	3.7	7.5	4.9	7.3	5.2	7.0	4.8	6.5	8.6	5.2
B	3.5	8.6	3.1	8.0	4.2	7.8	4.5	7.5	4.0	6.9	8.8	5.8
C	3.2	9.3	2.8	8.8	3.9	8.6	4.0	8.3	3.6	7.7	8.2	7.9
D	3.1	11.9	2.7	11.2	3.9	11.0	3.9	10.6	3.4	9.9	7.7	9.4

(b) P3, $n = 30$

	normal		Student t		gamma		log-normal		log-Student t		bootstrap BC_a	
	P_{05}	P_{95}	P_{05}	P_{95}	P_{05}	P_{95}	P_{05}	P_{95}	P_{05}	P_{95}	P_{05}	P_{95}
A	4.0	7.2	3.5	6.6	4.8	6.4	5.1	6.1	4.6	5.5	8.5	4.9
B	4.4	7.9	3.9	7.2	5.0	7.1	5.3	6.7	4.7	6.2	9.5	5.0
C	4.7	7.4	4.1	6.8	5.3	6.7	5.3	6.3	4.8	5.8	9.8	5.8
D	5.8	7.1	5.1	6.6	6.4	6.5	6.2	6.2	5.6	5.6	10.5	7.1

(c) GEV, C

	normal		Student t		gamma		log-normal		log-Student t		bootstrap BC_a	
	P_{05}	P_{95}	P_{05}	P_{95}	P_{05}	P_{95}	P_{05}	P_{95}	P_{05}	P_{95}	P_{05}	P_{95}
$n = 100$	3.7	8.9	3.5	8.6	4.2	8.3	4.4	8.1	4.2	7.9	7.0	6.8
$n = 50$	3.2	9.8	2.9	9.5	3.8	9.2	4.0	8.8	3.7	8.5	7.5	6.7
$n = 30$	3.2	9.3	2.8	8.8	3.9	8.6	4.0	8.3	3.6	7.7	8.2	7.9
$n = 10$	3.4	12.4	2.4	10.5	4.1	11.2	4.0	10.6	3.2	8.5	11.8	12.2

HESSD
7, 5467–5496, 2010

Table 2. Continued.

(d) P3, C

	normal		Student t		gamma		log-normal		log-Student t		bootstrap BC_a	
	P_{05}	P_{95}	P_{05}	P_{95}	P_{05}	P_{95}	P_{05}	P_{95}	P_{05}	P_{95}	P_{05}	P_{95}
$n = 100$	4.5	6.2	4.2	6.0	4.7	5.8	4.8	5.7	4.7	5.5	7.7	4.8
$n = 50$	4.6	6.7	4.3	6.4	5.3	6.2	5.3	5.9	5.0	5.6	8.6	5.0
$n = 30$	4.7	7.4	4.1	6.8	5.3	6.7	5.3	6.3	4.8	5.8	9.8	5.8
$n = 10$	5.6	10.1	4.6	8.4	6.5	9.0	6.1	8.5	5.0	6.6	13.2	8.7

(e) $n = 30$, A

	normal		Student t		gamma		log-normal		log-Student t		bootstrap BC_a	
	P_{05}	P_{95}	P_{05}	P_{95}	P_{05}	P_{95}	P_{05}	P_{95}	P_{05}	P_{95}	P_{05}	P_{95}
GEV	4.2	8.0	3.7	7.5	4.9	7.3	5.2	7.0	4.8	6.5	8.6	5.2
P3	4.0	7.2	3.5	6.6	4.8	6.4	5.1	6.1	4.6	5.5	8.5	4.9
LN	3.9	7.6	3.5	7.1	4.5	7.0	4.8	6.6	4.4	6.1	8.5	5.5
GP	7.0	4.7	6.4	4.2	7.6	4.1	8.0	4.0	7.2	3.5	10.1	3.2
GL	2.8	10.5	2.5	9.9	3.7	9.7	4.0	9.3	3.6	8.7	7.9	6.6

(f) $n = 30$, D

	normal		Student t		gamma		log-normal		log-Student t		bootstrap BC_a	
	P_{05}	P_{95}	P_{05}	P_{95}	P_{05}	P_{95}	P_{05}	P_{95}	P_{05}	P_{95}	P_{05}	P_{95}
GEV	3.1	11.9	2.7	11.2	3.9	11.0	3.9	10.6	3.4	9.9	7.7	9.4
P3	5.8	7.1	5.1	6.6	6.4	6.5	6.2	6.2	5.6	5.6	10.5	7.1
LN	3.6	9.7	3.1	9.2	4.2	9.1	4.1	8.6	3.7	7.9	8.3	8.9
GP	4.3	8.5	3.8	8.0	4.9	7.9	4.8	7.5	4.3	7.0	9.2	7.7
GL	3.0	13.0	2.7	12.3	3.7	12.1	3.7	11.5	3.3	10.6	7.1	10.2

HESSD
7, 5467–5496, 2010

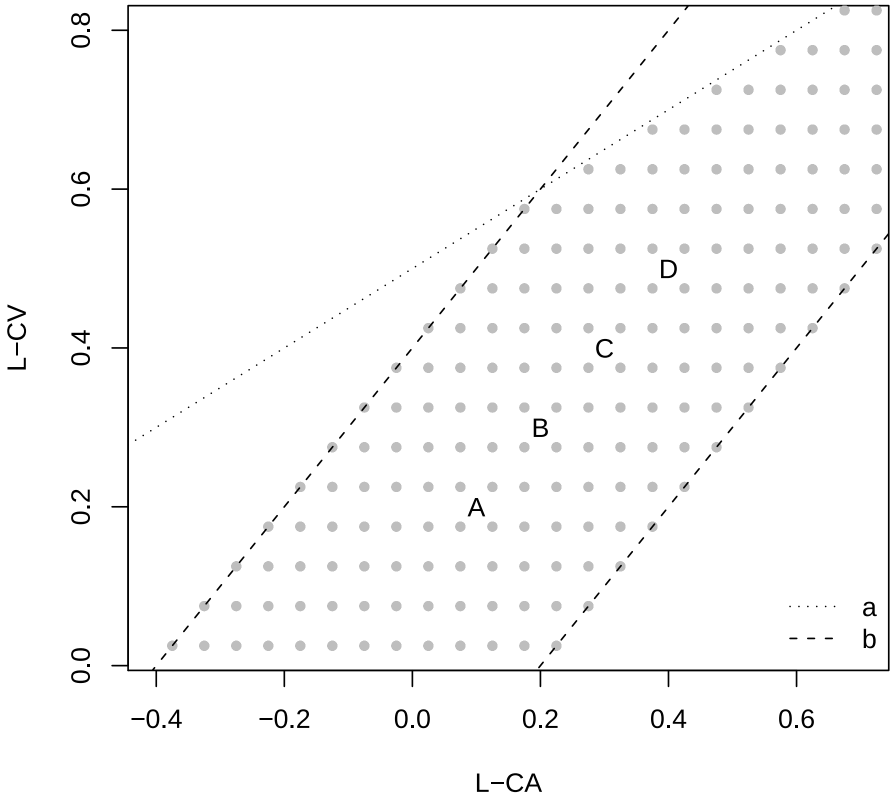

Fig. 1. L-CV - L-CA diagram. Lines are: **(a)** numerical constraint given by Hosking and Wallis (1997); **(b)** bisector band identified using Vogel and Wilson (1996) samples (see Viglione et al., 2007). Points A, B, C and D have L-CV = 0.2, 0.3, 0.4, 0.5 and L-CA = 0.1, 0.2, 0.3, 0.4 respectively.

HESSD
7, 5467–5496, 2010

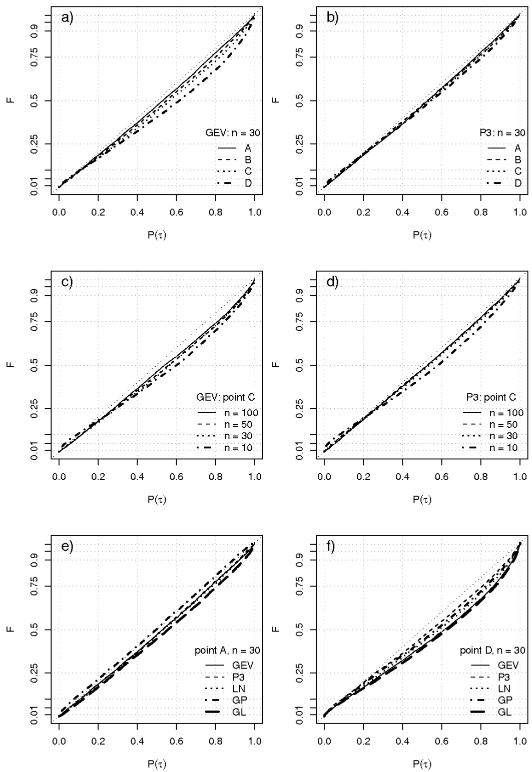

Fig. 2. Probability plot representation of $P(\tau)$ when assuming the log-Student t sampling distribution of Eq. (14) for t. Different situations are considered: **(a)** GEV parent distributions with different asymmetry (point A, B, C, D of Fig. 1); **(b)** P3 parent distributions with different asymmetry; **(c)** GEV parent distributions and samples of different length n; **(d)** P3 parent distributions and samples of different length n; **(e)** different parent distributions with low asymmetry (point A); **(f)** different parent distributions with high asymmetry (point D).

HESSD

7, 5467–5496, 2010

Title Page
Abstract | Introduction
Conclusions | References
Tables | Figures
◀I | ▶I
◀ | ▶
Back | Close
Full Screen / Esc
Printer-friendly Version
Interactive Discussion

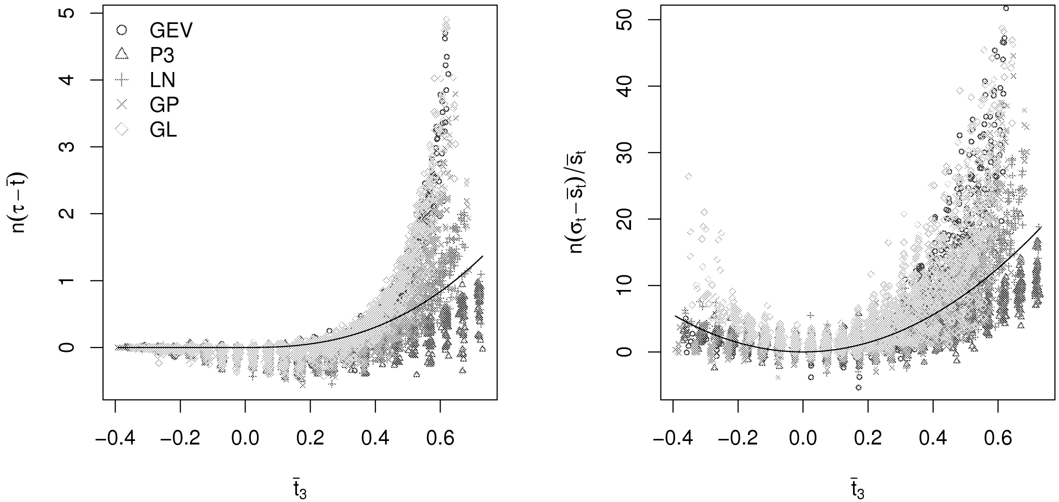

Fig. 3. Biases of t and s_t: **(a)** $n\cdot(\tau-\bar{t})$ vs the sample L-CA $\bar{t}_3$; **(b)** $n\cdot(\sigma_t-\bar{s}_t)/\bar{s}_t$ vs. the sample L-CA $\bar{t}_3$. Every point rises from 1000 simulated samples and corresponds to a gray point in Fig. 1. With continuous lines the proposed corrections of Eqs. (16) and (17) are indicated.

HESSD
7, 5467–5496, 2010

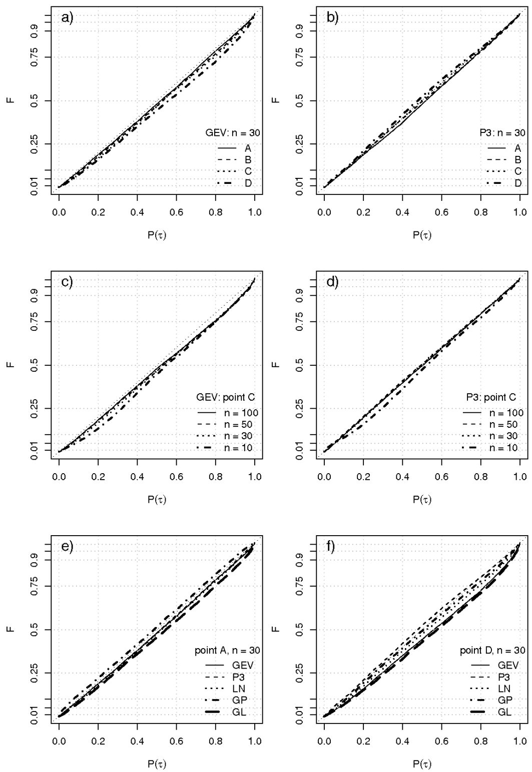

Fig. 4. Probability plot representation of $P(\tau)$ when assuming the log-Student t sampling distribution of Eq. (14) for t and applying the corrections of Eqs. (16) and (17). Different situations are considered: **(a)** GEV parent distributions with different asymmetry (point A, B, C, D of Fig. 1); **(b)** P3 parent distributions with different asymmetry; **(c)** GEV parent distributions and samples of different length n; **(d)** P3 parent distributions and samples of different length n; **(e)** different parent distributions with low asymmetry (point A); **(f)** different parent distributions with high asymmetry (point D).

HESSD
7, 5467–5496, 2010

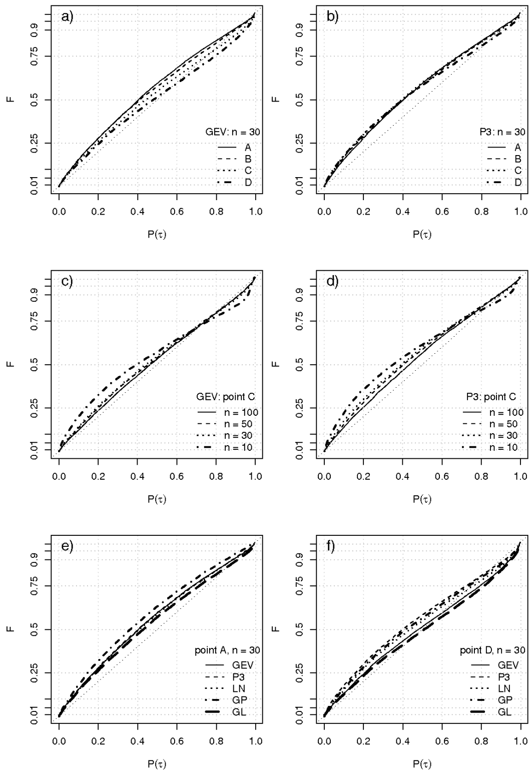

Fig. 5. Probability plot representation of $P(\tau)$ for different situations if the BC_a distribution is used (Eq. 18): **(a)** GEV parent distributions with different asymmetry (point A, B, C, D of Fig. 1); **(b)** P3 parent distributions with different asymmetry; **(c)** GEV parent distributions and samples of different length n; **(d)** P3 parent distributions and samples of different length n; **(e)** different parent distributions with low asymmetry (point A); **(f)** different parent distributions with high asymmetry (point D).

HESSD
7, 5467–5496, 2010

Sampling distribution of the coefficient of L-variation

A. Viglione

Title Page
Abstract Introduction
Conclusions References
Tables Figures
◀I ▶I
◀ ▶
Back Close
Full Screen / Esc
Printer-friendly Version
Interactive Discussion

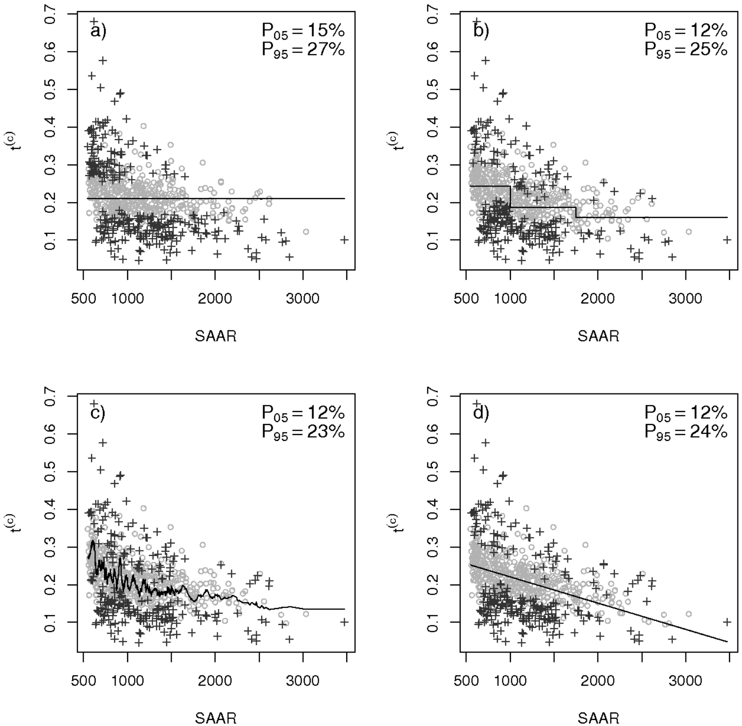

Fig. 6. Corrected L-CV $t^{(c)}$ (Eq. 16) versus mean annual precipitation SAAR in UK (data from the Flood Estimation Handbook, Robson and Reed, 1999). The black continuous line is the modeled regional value t^R; gray circles (∘) are sites for which the modeled t^R is inside the confidence interval of the sample L-CV with 10% significance level, when assuming the log-Student t sampling distribution of Eq. (14) for t and applying the corrections of Eqs. (16) and (17); black crosses (+) are sites for which it is outside of it. Four models are considered: **(a)** one unique region where $t^R = \bar{t}^{(c)}$; **(b)** three regions with different SAAR; **(c)** regions obtained with a simplified ROI approach; **(d)** linear regression model.

HESSD

7, 5467–5496, 2010